

High-resolution VUV-laser spectroscopic study of the  $B\ 1\Sigma^+_{(u)}(v = 0-2) \leftarrow X\ 1\Sigma^+_{(g)}(v' = 0)$   
Lyman bands in  $H_2$  and HD

This article has been downloaded from IOPscience. Please scroll down to see the full text article.

2006 J. Phys. B: At. Mol. Opt. Phys. 39 L195

(<http://iopscience.iop.org/0953-4075/39/8/L02>)

View [the table of contents for this issue](#), or go to the [journal homepage](#) for more

Download details:

IP Address: 38.107.179.214

The article was downloaded on 13/02/2012 at 22:02

Please note that [terms and conditions apply](#).

## LETTER TO THE EDITOR

# High-resolution VUV-laser spectroscopic study of the $B^1\Sigma_u^+(v' = 0-2) \leftarrow X^1\Sigma_g^+(v'' = 0)$ Lyman bands in $H_2$ and HD

U Hollenstein<sup>1</sup>, E Reinhold, C A de Lange and W Ubachs

Laser Centre, Vrije Universiteit, De Boelelaan 1081, 1081 HV Amsterdam, The Netherlands

E-mail: [wimu@nat.vu.nl](mailto:wimu@nat.vu.nl)

Received 13 February 2006, in final form 9 March 2006

Published 27 March 2006

Online at [stacks.iop.org/JPhysB/39/L195](http://stacks.iop.org/JPhysB/39/L195)**Abstract**

Spectroscopic measurements on the  $B^1\Sigma_u^+(v' = 0-2) \leftarrow X^1\Sigma_g^+(v'' = 0)$  Lyman bands in  $H_2$  and the  $B^1\Sigma^+(v' = 0-2) \leftarrow X^1\Sigma^+(v'' = 0)$  Lyman bands in HD are presented using a narrow bandwidth vacuum ultraviolet laser system combined with an accurate frequency calibration. These measurements complete the recently published data on the Lyman frequency transitions of Philip *et al* (2004 *Can. J. Chem.* **82** 713–22).

**1. Introduction**

$H_2$  is by far the most abundant molecule in the cosmos and its characteristic electronic systems, the  $B^1\Sigma_u^+ \leftarrow X^1\Sigma_g^+$  and  $C^1\Pi_u \leftarrow X^1\Sigma_g^+$  band systems, known as the Lyman and Werner bands, are the most prominent spectroscopic absorption features to be observed in outer space. Because the Earth's atmosphere is not transparent in the vacuum ultraviolet (VUV) and extreme ultraviolet (XUV) ranges, it took until 1970 for the first spectral recording of  $H_2$  in space using a rocket-borne spectrometer in the wavelength range between 100 nm and 110 nm [1]. Later a large number of lines in the VUV spectrum of molecular hydrogen was observed with the *Copernicus* satellite telescope [2]. The Hubble Space Telescope, equipped with a high-resolution XUV spectrometer, detected vibrationally excited molecular hydrogen in interstellar space, in the direction of  $\zeta$ -Ophiuchi [3]. Similarly the Galileo orbiter, also carrying an extreme ultraviolet spectrometer, recorded  $H_2$  spectra from the north and south polar regions of Jupiter [4]. Since 1999 the *Far-Ultraviolet Spectroscopic Explorer* is in orbit, detecting  $H_2$  from nearby and remote locations in the universe [5]. In all these observations, the Lyman bands are the prominent features under investigation.

In the past decade  $H_2$  absorption spectra of quasi-stellar objects have been recorded with ground-based telescopes; the high redshifts ( $z = 2-3$ ) allow for registering the Lyman

<sup>1</sup> Present address: Laboratory of Physical Chemistry, ETH Zurich, CH-8093 Zurich, Switzerland.

bands in the visible domain, where the light penetrates through the Earth's atmosphere. These observations are made in view of the possibility that the proton-to-electron mass ratio  $\mu = M_p/m_e$  has varied on a cosmological time scale [6–11]. Such observations allow for a comparison of spectra where the absorption has taken place some 12 Gyr ago, and spectra recorded in the laboratory in the modern epoch. The most stringent constraint on a possible variation of the proton-to-electron mass ratio following from such a comparison is  $\Delta\mu/\mu = (-0.5 \pm 3.6) \times 10^{-5}$  ( $2\sigma$ ) [12]. During these evaluations the need for extremely accurate zero-Doppler transition wavelengths in the Lyman and Werner band systems has emerged.

The Ottawa group around Herzberg performed a number of high-resolution absorption and emission studies on the Lyman bands [13–16], which were followed by the elaborate emission studies of the Meudon group at somewhat higher resolution [17, 18]. Baig and Connerade [19] performed an absorption study on  $H_2$  using synchrotron radiation, while Jungen *et al* [20] determined level energies for the B,  $v = 0$  and 1 states by cascaded infrared transitions, using Fourier-transform infrared (FTIR) spectroscopy. The Amsterdam group performed extensive wavelength calibration studies on the Lyman bands of  $H_2$  [21, 22] and HD [23], using a laser-based VUV source allowing for an absolute uncertainty of the transition frequencies of better than  $0.1 \text{ cm}^{-1}$ . Since the resolution of the Amsterdam VUV laser system was improved by a factor of 20 [24], investigations of the Lyman bands for  $v' = 2$ –18 could be performed, yielding absolute accuracies of  $10^{-7}$  or better [25]. In the latter study, problems were encountered generating wavelengths in the range from 105 nm to 110 nm. Moreover, in that range no saturated  $I_2$  lines, to be used for reference calibration [26, 27], were available. These issues have now been resolved and here we present accurate calibrations of Lyman lines in the range from 105 nm to 110 nm, for  $H_2$  as well as for HD.

## 2. Experiment

The experimental setup is described in the previous papers [24, 28] and is only summarized here. The tunable cw output of a 380 D Spectra Physics ring dye laser with Stabilok, which is operated with a 10 W Spectra Physics Millennia X Nd:YVO<sub>4</sub> laser as a pump laser and with DCM as a gain medium, is transmitted (via a single-mode optical fibre) into a pulsed dye amplifier, pumped by a seeded Spectra Physics Nd:YAG laser (GCR-5, repetition rate 10 Hz) and producing nearly Fourier-transform limited laser pulses with a length of about 5 ns. The pulsed amplification consists of three dye cells operated with DCM. The amplified laser beam is frequency doubled using a KD\*P crystal. The UV beam (1–2 mJ per pulse) is separated into two beams by placing a metallic needle at the centre of the laser beam. The two UV beams are focused into a vacuum chamber. The VUV is produced at the focus of the UV beam in a pulsed supersonic gas expansion of xenon using a piezo-disc home-built pulsed valve (design described in [29]) with a stagnation pressure of approximately 4 bar. After frequency tripling, the VUV beam, which has a bandwidth of  $\Gamma \approx 250 \text{ MHz}$  [28], is located spatially between the two fundamental UV beams. The VUV beam is led through an adjustable slit and crossed perpendicularly with a pulsed, skimmed probe gas beam originating from a supersonic gas expansion using a General valve nozzle (series 9, 0.8 mm orifice) with a stagnation pressure of approximately 1 bar. The  $H_2$  or HD probe gases are seeded with xenon in a 1:3 mixture ( $H_2/HD:Xe$ ) or used in a pure form. The distance between the probe gas nozzle and the used skimmer (opening 2 mm) is typically 60 mm.

The  $H_2/HD$  spectra are monitored by 1+1' REMPI using the fourth harmonic of an unseeded Spectra Physics Nd:YAG laser (GCR-4, 266 nm, approx. 10 mJ per pulse) for the ionization step, and by applying a pulsed electric field (triggered after the laser pulse so that

**Table 1.** Error budget of the overall uncertainty in the calibration procedure.

Source	$\sigma^a$ (MHz)
Doppler uncertainty <sup>b</sup>	60–100
AC Stark shift	30–50
Chirp shift	100
I <sub>2</sub> calibration	10
Étalon drift	2
Statistics	80
Resulting uncertainty <sup>c</sup>	145–170

<sup>a</sup>  $\sigma$  stands for standard deviation.

<sup>b</sup> Estimated Doppler uncertainty at 91 000 cm<sup>-1</sup> for pure H<sub>2</sub>.

<sup>c</sup> Calculated as the square root of the sum of all specified uncertainties above.

laser excitation is performed under field-free conditions) to accelerate the ions towards an electron multiplier (Thorn EMI) detector. The distance between the interaction region and the ion detector is used as a time-of-flight mass spectrometer (perpendicular to both the VUV beam and the probe gas beam). The ion signal is recorded using a boxcar integrator (Stanford Research) to measure the area under a specific  $m/z$  peak in the time-of-flight mass spectrum. The signal is then transferred to a measuring program on a personal computer.

Possible effects of Doppler-induced shifts of the resonance frequency as a result of non-perpendicular alignment of the VUV and molecular beams is assessed by comparing spectral measurements obtained from pure hydrogen and from hydrogen/xenon mixtures, for which the molecular beam velocities are different. Furthermore it is noted that the interaction volume of the overlapping VUV/UV laser beams and the molecular beam is rather large, with the light beams possessing a diameter of 8 mm. Hence the AC-Stark induced shift of the ionizing UV beam is kept to a minimum. Finally there is the effect of frequency chirp in the dye amplifiers, which may result in a net shift between the centre frequency of the VUV beam used in the experiment, and the fundamental frequency (multiplied by a factor of 6) of the ring-dye laser, used for frequency calibration. All three issues are extensively discussed in the previous papers [24, 25] and similar procedures are followed to estimate resulting uncertainties associated with these systematic effects.

The VUV frequency is calibrated, using a fraction of the ring dye laser output to measure a Doppler-free absorption spectrum of molecular iodine and another fraction to record simultaneously an étalon transmission spectrum. The étalon is actively locked to a transmission mode of a frequency stabilized HeNe laser (Newport, model NL-1). The stability of the HeNe laser in the locked mode was measured with a fs frequency comb [30] and determined to be better than 2 MHz within a 20 min laser scan. The reference data for calibration were derived from a calculation of the iodine hyperfine structure by the IodineSpec program<sup>2</sup> An error budget of the calibration procedure is listed in table 1.

### 3. Results

The spectroscopic results are summarized in table 2 for the B <sup>1</sup>Σ<sub>u</sub><sup>+</sup> ( $v' = 0-2$ ) ← X <sup>1</sup>Σ<sub>g</sub><sup>+</sup> ( $v'' = 0$ ) Lyman bands in H<sub>2</sub> and in table 4 for the B <sup>1</sup>Σ<sup>+</sup> ( $v' = 0-2$ ) ← X <sup>1</sup>Σ<sup>+</sup> ( $v'' = 0$ )

<sup>2</sup> The reference data for calibration were derived from a calculation of the iodine hyperfine structure by the IodineSpec program; see [31].

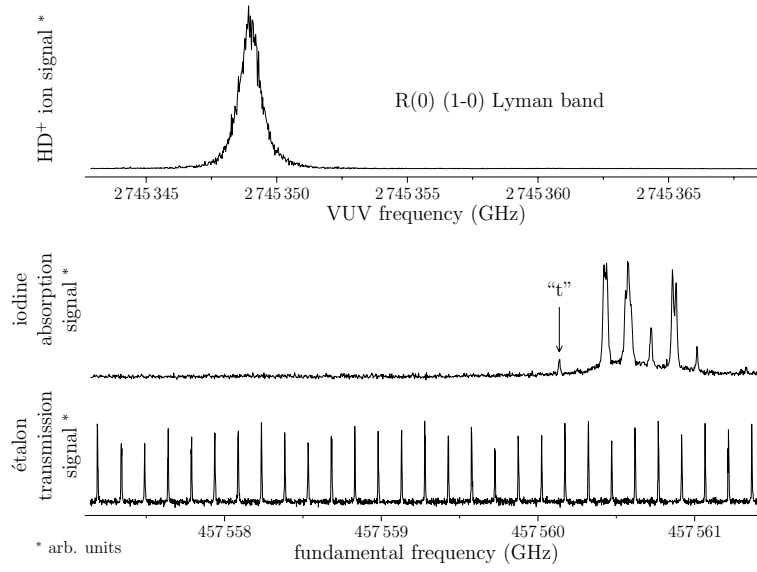


**Figure 1.** A spectrum of the  $B^1\Sigma^+(v' = 1) \leftarrow X^1\Sigma^+(v'' = 0)$  R(0) Lyman transition in HD (upper trace). The linewidth of the measured transition is 900(25) MHz with a significant Doppler contribution. The lower two traces represent a simultaneously recorded Doppler-free calibration spectrum in molecular iodine (using the R(42) (5–5) transition with the ‘t’-component at 15 262.563 29  $\text{cm}^{-1}$ ) and an étalon transmission spectrum of a frequency stabilized étalon (lower trace).

**Table 2.** Transition wavenumbers of the Lyman bands in  $\text{H}_2$  for  $v' = 0\text{--}2$  with uncertainties given in parentheses ( $1\sigma$ ). The values in the last three columns are in comparison with the reference values.

$\text{H}_2 B^1\Sigma_u^+(v', J') \leftarrow \text{H}_2 X^1\Sigma_g^+(v'' = 0, J'')$					
$v'$		$\frac{E_{\text{exp}}}{hc}$ ( $\text{cm}^{-1}$ ) This work	$\frac{E_{\text{exp}} - E_{\text{ref}}}{hc}$ ( $\text{cm}^{-1}$ )		
			[19] <sup>a</sup>	[18] <sup>b</sup>	[20] <sup>c</sup>
0	P(1)	90 085.0166 (50)		−0.0534	−0.0035
	R(0)	90 242.3373 (57)		0.0273	−0.0067
	R(1)	90 201.1545 (57)		−0.0255	−0.0046
1	P(1)	91 403.3354 (50)	0.1154	−0.0146	−0.0107
	P(2)	91 204.3491 (53)	1.1291	−0.0209	−0.0155
	P(3)	90 926.6825 (57)	0.1525	−0.0475	−0.0102
	R(0)	91 558.7222 (53)	−0.0878	0.0022	−0.0158
	R(1)	91 513.7115 (48)	0.0215	−0.0585	−0.0136
	R(2)	91 387.2454 (53)	−0.2146	−0.0346	−0.0352
2	R(3)	91 180.5323 (50)	0.0723	−0.0377	−0.0084
	R(2)	92 659.0480 (53)	−0.1320	0.0080	
	R(3)	92 446.1132 (57)	0.0432	−0.0368	
	R(4)	92 153.5373 (53)	−0.2127	−0.0127	

<sup>a</sup> Uncertainties in [19] are specified as  $\pm 0.003 \text{ \AA}$  at about 1100  $\text{\AA}$ , which correspond to an uncertainty of approx.  $0.25 \text{ cm}^{-1}$ .

<sup>b</sup> Calculated using the level energies given in [18] (table VI). The ground-state levels are taken from [15] (table 5). The specified uncertainties in [18] are less than  $0.1 \text{ cm}^{-1}$ .

<sup>c</sup> Calculated using the level energies given in [20] (table I). The ground-state levels are calculated using the values of [32] (table 2, column B). The specified uncertainties in [20] are in the range of  $\pm 0.005 \text{ cm}^{-1}$ .

**Table 3.** Comparison of the difference frequencies of  $R(J'') - P(J'' + 2)$  for  $J'' = 0$  and  $J'' = 1$  of the Lyman transitions in  $H_2$  for  $(v', v'') = (1, 0)$  (see table 2) and the  $S(J'')$  transitions in the  $X^1\Sigma_g^+$  ground state of  $H_2$  (see [32]).

$J''$	$R(J'') - P(J'' + 2)$ ( $cm^{-1}$ )	$S(J'')$ ( $cm^{-1}$ )
	This work	[32]
0	354.373 (7)	354.3734 (2)
1	587.029 (7)	587.0325 (2)

**Table 4.** Transition wavenumbers of the Lyman bands in HD for  $v' = 0-2$  with uncertainties given in parentheses ( $1\sigma$ ). The reference data are taken from Dabrowski and Herzberg [16] using the values of table 10 for the  $B^1\Sigma^+$  excited state of HD and from Evenson *et al* [33] and Ulivi *et al* [34] for the  $X^1\Sigma^+$  ground state.

HD $B^1\Sigma^+(v', J') \leftarrow HD X^1\Sigma^+(v'' = 0, J'')$			
$v'$		$\frac{E}{hc}$ ( $cm^{-1}$ )	$\frac{E_{exp} - E_{ref}}{hc}$ ( $cm^{-1}$ )
0	P(1)	90 310.3785 (52)	-0.2536
	R(0)	90 428.9498 (46)	-0.2482
	R(1)	90 398.1855 (44)	-0.2445
	R(2)	90 307.5060 (44)	-0.2324
1	P(1)	91 457.7087 (44)	-0.1534
	P(2)	91 307.9139 (46)	-0.1545
	P(3)	91 098.5843 (45)	-0.1476
	R(0)	91 574.9856 (48)	-0.1525
	R(1)	91 541.6650 (45)	-0.1498
	R(2)	91 447.2193 (44)	-0.1319
2	R(3)	91 292.3011 (44)	-0.0861
	P(2)	92 425.8509 (44)	-0.2501
	R(0)	92 692.9203 (52)	-0.2503
	R(1)	92 657.4022 (52)	-0.2659

Lyman bands in HD. The upper trace in figure 1 shows the spectrum of the the  $B^1\Sigma^+(v' = 1, J' = 1) \leftarrow X^1\Sigma^+(v'' = 0, J'' = 0)$  transition in HD. The lower two traces represent the calibration spectra consisting of a Doppler-free absorption spectrum of molecular iodine (the B-X system) and a transmission spectrum of an étalon.

In table 3, the differences  $R(J'') - P(J'' + 2)$  for  $J'' = 0$  and  $J'' = 1$  of the  $B^1\Sigma_u^+(v' = 1) \leftarrow X^1\Sigma_g^+(v'' = 0)$  Lyman transitions are compared with the corresponding  $S(J'')$  transitions in the  $X^1\Sigma_g^+$  ground state of  $H_2$ . The values are consistent with the literature values of Jennings *et al* [32, 35]. This result provides an independent validation of the calibration procedures followed in the present study.

In the previous study by Philip *et al* [25], a value of  $92\,659.092(4)\,cm^{-1}$  was reported for the R(2) line of the B-X (2,0) Lyman band, largely disagreeing with the present value. We note here that in [25] the very weak R(2) line was only detected in an overview scan and that its uncertainty was largely underestimated. The present value, listed in table 2, has a properly estimated uncertainty and should be regarded as the true value.

#### 4. Conclusions

We present newly measured data of the Lyman transition of  $H_2$  and HD in the lowest vibrational states of the  $B^1\Sigma_u^+$  state ( $v' = 0-2$ ) including an accurate calibration using Doppler-free

absorption spectroscopy. These measurements complete the recently published data set on the Lyman frequency transitions of Philip *et al* [25].

Comparisons of the experimental transition wavenumbers with reference data are listed in table 2 for H<sub>2</sub> and in table 4 for HD. In the case of H<sub>2</sub> we obtain an average deviation of (A) 0.089 cm<sup>-1</sup>, (B) -0.026 cm<sup>-1</sup> and (C) -0.012 cm<sup>-1</sup> with respect to the reference data of (A) Baig and Connerade [19], measured by synchrotron spectroscopy, (B) Abgrall *et al* [18] and (C) Jungen *et al* [20], deduced from level energies. For HD, we compared our data with the values of Dabrowski and Herzberg [16] and obtain an average deviation of -0.19 cm<sup>-1</sup>.

The present values on the transition frequencies are substantially more accurate than the previously published data and may find application in a number of astrophysical studies. The values are of high importance in particular for the comparison with transition frequencies of hydrogen lines observed in high-redshifted quasi-stellar objects.

## Acknowledgments

We thank Dr Horst Knöckel from Hannover for providing information about calibration data on molecular iodine. UH acknowledges the European Union for a Postdoctoral fellowship from the RTN network on Reactive Intermediates (HPRN-CT-2000-00006).

## References

- [1] Carruthers G R 1970 Rocket observation of interstellar molecular hydrogen *Astrophys. J.* **161** L81–L85
- [2] Morton D C and Dinerstein H L 1976 Interstellar molecular hydrogen toward zeta Puppis *Astrophys. J.* **204** 1–11
- [3] Federman S R, Cardelli J A, van Dishoeck E F, Lambert D L and Black J H 1995 Vibrationally excited H<sub>2</sub>, HCl, and NO<sup>+</sup> in the diffuse clouds toward ζ Ophiuchi *Astrophys. J.* **445** 325–9
- [4] Ajello J *et al* 1998 Galileo orbiter ultraviolet observations of Jupiter aurora *J. Geophys. Res.* **103** 20125–48
- [5] Moos H W *et al* 2000 Overview of the Far Ultraviolet Spectroscopic Explorer Mission *Astrophys. J.* **538** L1–L6
- [6] Varshalovich D A and Levshakov S A 1993 On a time-dependence of physical constants *JETP Lett.* **58** 237–40
- [7] Varshalovich D A and Potekhin A Y 1995 Cosmological variability of fundamental physical constants *Space Sci. Rev.* **74** 259–68
- [8] Cowie L L and Songaila A 1995 Astrophysical limits on the evolution of dimensionless physical constants over cosmological time *Astrophys. J.* **453** 596–8
- [9] Ivanchik A V, Rodriguez E, Petitjean P and Varshalovich D A 2002 Do the fundamental constants vary in the course of cosmological evolution? *Astron. Lett.* **28** 423–7
- [10] Potekhin A Y, Ivanchik A V, Varshalovich D A, Lanzetta K M, Baldwin J A, Williger G M and Carswell R F 1998 Testing cosmological variability of the proton-to-electron mass ratio using the spectrum of PKS 0528-250 *Astrophys. J.* **505** 523–8
- [11] Levshakov S A, Dessauges-Zavadsky M, D'Odorico S and Molaro P 2002 A new constraint on cosmological variability of the proton-to-electron mass ratio *Mon. Not. R. Astron. Soc.* **333** 373–7
- [12] Ubachs W and Reinhold E 2004 Highly accurate H<sub>2</sub> Lyman and Werner band laboratory measurements and an improved constraint on a cosmological variation of the proton-to-electron mass ratio *Phys. Rev. Lett.* **92** 101302
- [13] Herzberg G and Howe L L 1959 The Lyman bands of molecular hydrogen *Can. J. Phys.* **37** 636
- [14] Dabrowski I and Herzberg G 1974 Absorption-spectrum of D<sub>2</sub> from 1100 to 840 Å *Can. J. Phys.* **52** 1110
- [15] Dabrowski I 1984 The Lyman and Werner bands of H<sub>2</sub> *Can. J. Phys.* **62** 1639–64
- [16] Dabrowski I and Herzberg G 1976 Absorption and emission-spectra of HD in vacuum ultraviolet *Can. J. Phys.* **54** 525–67
- [17] Abgrall H, Roueff E, Launay F, Roncin J-Y and Subtil J-L 1993 Table of the Lyman band system of molecular hydrogen *Astron. Astrophys. Suppl. Ser.* **101** 273–321
- [18] Abgrall H, Roueff E, Launay F, Roncin J-Y and Subtil J-L 1993 The Lyman and Werner band systems of molecular hydrogen *J. Mol. Spectrosc.* **157** 512–23
- [19] Baig M A and Connerade J P 1985 New high-resolution photoabsorption study of the Lyman bands of H<sub>2</sub> *J. Phys. B: At. Mol. Phys.* **18** L809–L813

- [20] Jungen Ch, Dabrowski I, Herzberg G and Vervloet M 1990 High orbital angular momentum states in H<sub>2</sub> and D<sub>2</sub>: III. Singlet–triplet splittings, energy levels, and ionization potentials *J. Chem. Phys.* **93** 2289–98
- [21] Hinnen P C, Hogervorst W, Stolte S and Ubachs W 1994 Sub-Doppler laser spectroscopy of H<sub>2</sub> and D<sub>2</sub> in the range 91–98 nm *Can. J. Phys.* **72** 1032–42
- [22] Reinhold W, Hogervorst W and Ubachs W 1996 High resolution laser spectroscopy of H<sub>2</sub> at 86–90 nm *J. Mol. Spectrosc.* **180** 156–63
- [23] Hinnen P C, Werners S E, Stolte S, Hogervorst W and Ubachs W 1995 XUV-laser spectroscopy of HD at 92–98 nm *Phys. Rev. A* **52** 4425–33
- [24] Eikema K S E, Ubachs W, Vassen W and Hogervorst W 1997 Lamb shift measurement in the 1 <sup>1</sup>S ground state of helium *Phys. Rev. A* **55** 1866–84
- [25] Philip J, Sprengers J P, Pielage Th, de Lange C A, Ubachs W and Reinhold E 2004 Highly accurate transition frequencies in the H<sub>2</sub> Lyman and Werner absorption bands *Can. J. Chem.* **82** 713–22
- [26] Velchev I, van Dierendonck van, Hogervorst W and Ubachs W 1998 A dense grid of reference iodine lines for optical frequency calibration in the range 571–596 nm *J. Mol. Spectrosc.* **187** 21–7
- [27] Xu S C, van Dierendonck R, Hogervorst W and Ubachs W 2000 A dense grid of reference iodine lines for optical frequency calibration in the range 595–655 nm *J. Mol. Spectrosc.* **201** 256–66
- [28] Ubachs W, Hinnen P C and Reinhold E 1997 Observation of inter-Rydberg transitions in H<sub>2</sub> coinciding with diffuse interstellar bands *Astrophys. J.* **476** L93–L96
- [29] Proch D and Trickl T 1989 A high-intensity multi-purpose piezoelectric pulsed molecular beam source *Rev. Sci. Instrum.* **60** 713–6
- [30] Witte S, Zinkstok R Th, Ubachs W, Hogervorst W and Eikema K S E 2005 Deep-ultraviolet quantum interference metrology with ultrashort laser pulses *Science* **307** 400–3
- [31] Knöckel H, Bodermann B and Tiemann E 2004 High precision description of the rovibronic structure of the I<sub>2</sub> B–X spectrum *Eur. Phys. J. D* **28** 199–209
- [32] Jennings D E, Bragg S L and Brault J W 1984 The  $v = 0 \rightarrow 0$  spectrum of H<sub>2</sub> *Astrophys. J.* **282** L85–L88
- [33] Evenson K M, Jennings D A, Brown J M, Zink L R, Leopold K R, Vanek M D and Nolt I G 1988 Frequency measurement of the  $J = 1 \leftarrow 0$  rotational transition of HD *Astrophys. J.* **330** L135–L136
- [34] Ulivi L, de Natale P and Inguscio M 1991 Pure rotational spectrum of hydrogen deuteride by far-infrared Fourier-transform spectroscopy *Astrophys. J.* **378** L29–L31
- [35] Jennings D E and Brault J W 1983 The ground state of molecular hydrogen *J. Mol. Spectrosc.* **102** 265–72